www.czasopisma.pan.pl PAN POLSKA AKADEMIA NAUK www.journals.pan.pl

Arch. Metall. Mater., Vol. 61 (2016), No 2, p. 785–790

DOI: 10.1515/amm-2016-0132

M. KRUPIŃSKI*,#, K. LABISZ*, T.TAŃSKI*, B. KRUPIŃSKA*, M. KRÓL*, M. POLOK-RUBINIEC*

INFLUENCE OF Mg ADDITION ON CRYSTALLISATION KINETICS AND STRUCTURE OF THE Zn-Al-Cu ALLOY

In this work the effect of Mg addition on structure as well as kinetics of crystallisation of Zn-Al-Cu cast alloy was presented. To the zinc alloy was added 0.1% mass of Mg. The alloy was cast into a metal mould. Thermo-derivative analysis was performed using the UMSA platform (Universal Metallurgical Simulator and Analyzer). The investigated alloys were freely cooled down with a rate of 0.1°C s^{-1}. For the structure analysis were used results obtained using light microscopy, scanning and transmission electron microscopy.

Keywords: Casting, metallography, modification, cast zinc alloys, microstructure

1. Introduction

The properties of cast alloy depend on many factors. The most important is the chemical composition, because each of the elements affects individually or the components increase (eventually decrease) their mutual influence on structure and properties of alloy. A significant influence on the properties of cast alloys have external conditions, such as centrifugal force, metalostatic pressure as well as carried out modifications [1].

The exact knowledge of the effect of cooling rate of mould casting on the structure and temperature of phase transformations during crystallization equilibrium allows optimal control of the production process, therefore in this study was used the thermos-derivative analysis which allows to describe the phenomena that occur in the material during solidification, as well as due to changes in the chemical composition in the form of addition of Mg. The paper determines the effect of the addition of magnesium on the value of the temperature of begin (TDN) and end (TSol) of the alloy crystalisation. Also the solid fraction versus temperature solidification of the alloy was determined [2-4].

The shape of the differential curve defines to basic functions allows accurate calculation of latent crystallization heat of various phases crystallising during solidification [5, 6].

Assuming that the latent crystallization heat is proportional to the share of the various phases in the alloy, the thermo-derivative analysis also allows the calculation of the amount crystallized phases. Calculation of the above-mentioned properties is based on the characteristic points determined in a differential curve [7].

These points are usually reflecting the thermal effects occurring in the melt during crystallization, and are dependent on the alloy composition, cooling rate, heat generation rate, and crystallization temperature of the molten metal, and so the parameters affecting the final structure of the resulting alloy. These parameters characterize also the crystallization kinetics of the alloys [8].

Investigations carried out in work [9] indicate, that the difference in the morphology of the phase components are depending on the chemical composition. The investigated alloys are characterized by a solidification of Al, Zn and phases MgZn2, Mg2Zn11. These results are consistent with the results obtained in [10], where was presented graphically the Al-Mg-Zn reaction sequence during solidification. These corresponds in satisfactory way with their DTA/DSC (derivative thermos-analysis/ derivative scanning calorimetry) data. Computed constant-temperature contours on the liquidus and solidus surfaces of (Al) and found good agreement with the experimental results. A partial liquidus surface computed for alloys up to 30 mass% each of Al and Zn was compared with the present and the previous experimental results. Vertical sections computed at 5, 10, 15, 20, 25, and 30 mass% of Zn and at Al/Zn ratio of 1:1 were compared with the experimental data in the literature (Fig. 1, 2) [11].

The result of the undertaken research is to determine the relationship between the crystallization kinetics, microstructure, and functional properties of both unmodified and modified cast zinc magnesium alloys.

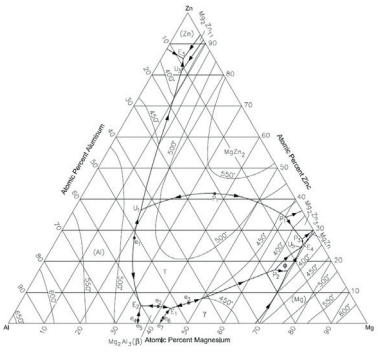

Fig. 1. Al-Mg-Zn computed liquidus projection [12]

* SILESIAN UNIVERSITY OF TECHNOLOGY, INSTITUTE OF ENGINEERING MATERIALS AND BIOMATERIALS, 18A KONARSKIEGO STR., 44-100 GLIWICE, POLAND

Corresponding author: Mariusz.Krupinski@polsl.pl

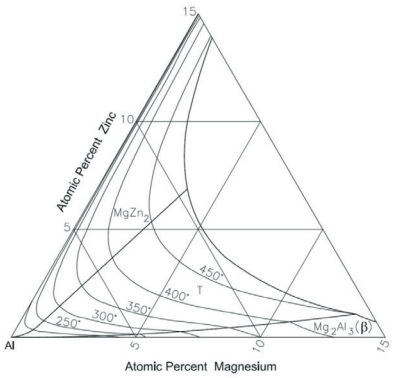

Fig. 2. Al-Mg-Zn solvus of the (Al) solid solution [12]

2. Experimental conditions

In order to determine the relationship between the crystallization kinetics of the alloy, and the chemical composition and microstructure, the casting were further modified with 0.1% mas. Mg, which chemical composition is presented in table 1 and the following tests were performed:

- thermo-derivative analysis of the investigated Zn alloys tested before and after modification with cooling rates at the temperature range of T_L and T_{Sol} 0.1°C s^{-1} (freely cooled alloy). Study of the effect of Mg addition was performed by means of a crystallization process simulation with UMSA using cylindrical specimens melted in a graphite crucible. For temperature measurement a chromel-alumel thermocouple of the K type was applied with a reaction time of 250 milisecond. Following the samples were used for thermo-derivative analysis were prepared with Ø30 mm in diameter and a height of 35mm. There are also made holes in the samples for thermocouples, in the place where a thermal centre for this type of sample geometry can occur.

The investigated samples have a mass of 160 g ± 5 g:

- macrostructure using light microscopy,
- microstructure using scanning electron microscope Zeiss Supra 35 equipped with EDS,
- the examinations of thin foils microstructure and phase identification were made on a high resolution transmission electron microscope Titan 80-300 in the scanning mode S\TEM.

TABLE 1

Chemical composition

Determination of zinc alloy	The mass concentration of alloying elements, %			
	Al	Cu	Mg	Zn
Zn-Al-Cu	10.02	0.98	-	rest
Zn-Al-Cu(0.1Mg)	8.25	0.76	0.1	rest

3. Results and discussion

The metallographic investigations results made on the light microscopy as well as studies carried out using scanning electron microscopy (SEM) show that the hypereutectic zinc alloys with aluminium and have the structure consisting of the solid α' solution (solution of zinc in aluminium matrix), and grains of α' + η eutectic, which morphology depends on the rate of the applied cooling. Examples of microstructure images which is composed of globular "monotectic" areas and α' + η eutectic with a morphology dependent on the cooling conditions, are presented in Fig. 3. The addition of 0.1 weight % of Mg changes the structure, which is characterized by precipitates of α ' phase and eutectic with changed morphology compared to the alloys without Mg as well as Zn precipitated (Fig. 4).

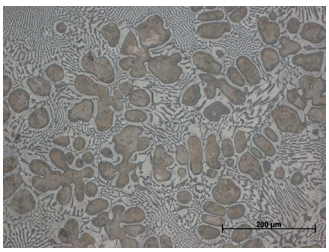

Fig. 3. Structure of the Zn-Al-Cu alloy, cooling rate of 0.1°C s^{-1}, etched in 10% HF solution

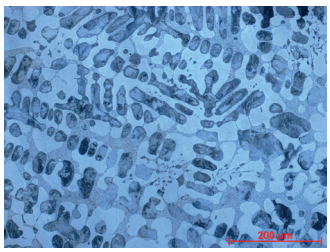

Fig. 4. Structure of the Zn-Al-Cu(0.1Mg) alloy, cooling rate of 0.1°C s^{-1}, etched in 10% HF solution

In the analysed monotectic areas was confirmed an average content of Zn and Al characteristic for eutectic (Figs. 5 and 6).

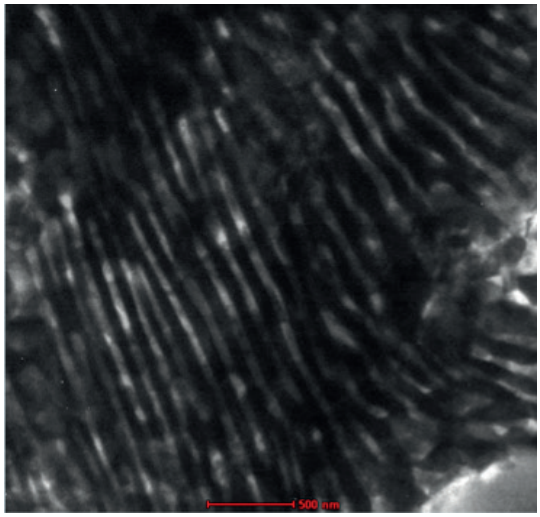

Fig. 5. Structure of the alloy cooled with 0.1°C s^{-1} the Zn-Al „monotectics"; EDS spectrum of the entire area is showed in Fig. 6

Observations made by scanning electron microscope and analysis of the chemical composition carried out using EDS quantitative microanalysis confirm the presence of magnesium in the eutectic are of the alloy (Fig. 7). It is worth to note that the characteristic element radiation in the EDS analysis derive from a larger volume of material than would indicate by the electron beam diameter, mainly due to the beam penetration into the material and to disperse of it through the sample surface depending on the electron energy, and this results in obtaining of characteristic radiation from bigger volume of the material (Fig. 8).

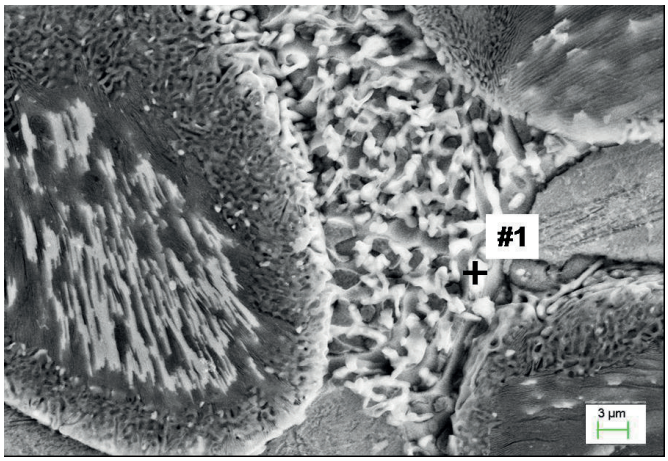

Fig. 7. Structure of the Zn-Al-Cu(0.1Mg) cast alloy, cooled at a rate of 0.1°C s^{-1}; EDS spectrum of the entire area shown in Fig. 8

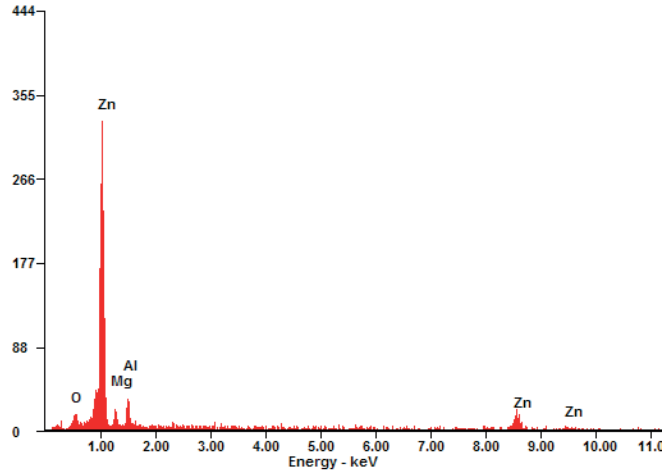

Fig. 8. EDS analysis preformed in the point #1 presented on Fig. 7

Transmission electron investigations reveals the microstructure of the investigated alloys in microscale. On Fig. 9 can be recognised the structure of the Zn-Al-Cu(0.1Mg) alloy. There can be especially determined the size of the crystallites present in the structure (Fig. 9a, 9b, 9c) which is in the range between 100 and 200 nm. The EDS microanalysis carried out allows to state, that the Mg addition is also dissolved in the Zn matrix Fig 9d. Also the performed diffraction pattern Figs 9e and 9f corresponding the bright field images confirm the polycrystalline nature of the alloy structure. Also the calculated d-pacing for the planes can be presented as 3.5% higher for the a=0.2665 nm d-spacing and, 5.2% higher for the c=0.4947 d-spacing

In contrast to the Zn-Al-Cu alloys (Fig. 11) the modification with magnesium and the determination the crystallization process, including the characteristic thermal changes indicating formation of multi-compound eutectics (Fig. 10, points IV), which crystallization starts at the temperature TEW (Al+Zn+Mg) and continues to achieve the solidus temperature TSol (point IV, Fig. 10). It is worth to note that each modification of the Zn-Al-Cu alloy with magnesium lowers both the temperature at the alloy crystallisation begin TL as well as crystallistaion begin of the eutectic α+η (Al+Zn), it causes also decrease of the temperature of the crystallization end TSol (Table 2).

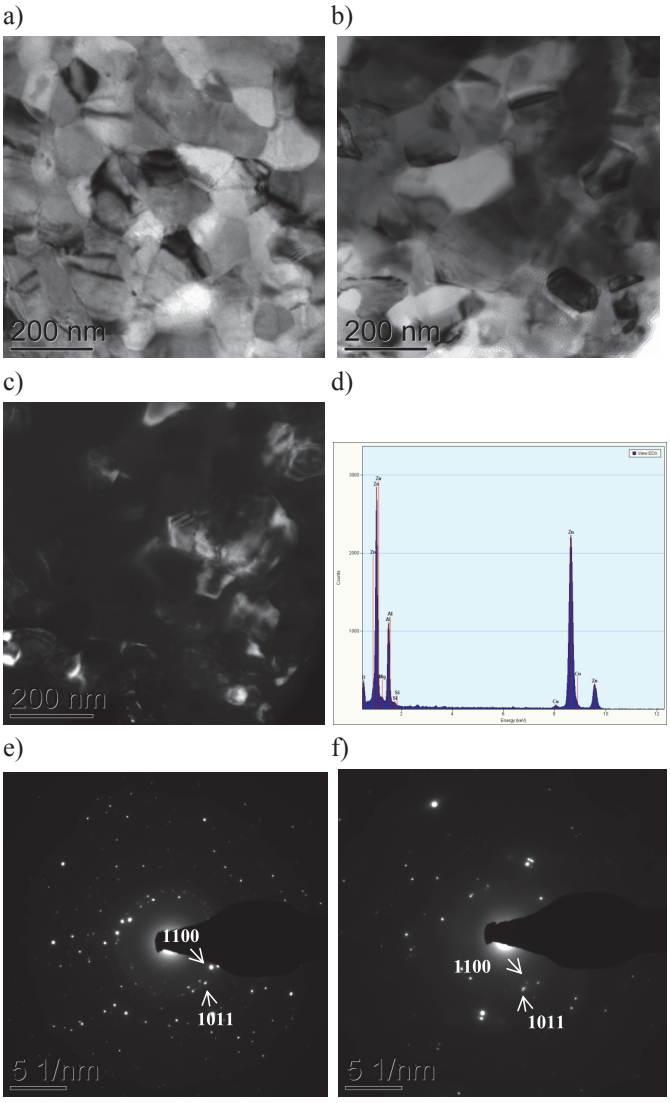

Fig. 9. Microstructure of the Zn-Al-Cu(0.1Mg) alloy, bright field, TEM area 1 a), bright field, TEM area 2 b), dark field, TEM area 2 c), EDS analysis of the entire place presented in area 1, d), diffraction pattern of area 1 e), diffraction pattern of area 2 f)

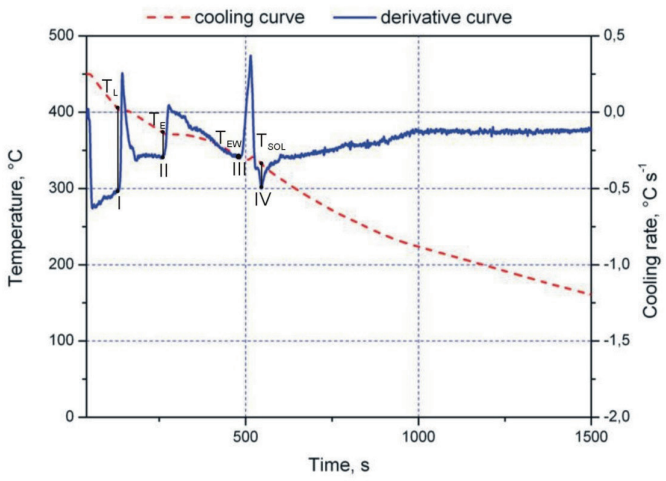

Fig. 10. The cooling curve and crystallization curve of the Zn-Al-Cu(0.1Mg) alloy, cooled at a rate of 0.1°C s^{-1}

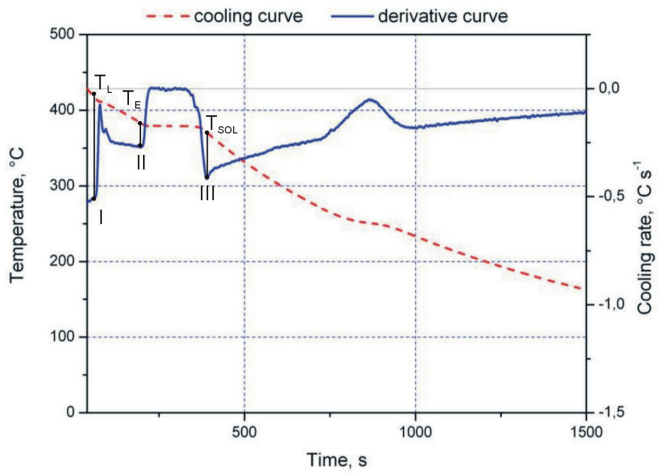

Fig. 11. The cooling curve and crystallization curve of the Zn-Al-Cu alloy, cooled at a rate of 0.1°C s^{-1}

TABLE 2

Characteristic temperature of the different stages of phase transformation during the Zn-Al-Cu and Zn-Al-Cu(0.1Mg) alloy crystallization, cooling rate of 0.1°C s^{-1}

Alloy	Temperature, °C			
	TL	TE	TEW	TSol
Zn-Al-Cu	414.5	381.2	-	372.7
Zn-Al-Cu(0.1Mg)	403.2	376.5	340.2	339.9

In tables 3 and 4 there are shown the calculated heat capacity values in the liquid state Cp_l, heat capacity in the solid state Cp_s, latent crystallization heat of the components, and their percentage.

Fig. 12 shows the fraction solid during the crystallization of individual components of the alloys: Zn-Al-Cu, and Zn-Al-Cu(0.1Mg), cooled at a rate of 0.1°C s^{-1}. There is a clear change in the fraction solid curve for alloys containing 0.1% mass. Mg addition, both in the initial crystallization stage as well as in its final phase, which can be associated with multi-phase eutectic solidification.

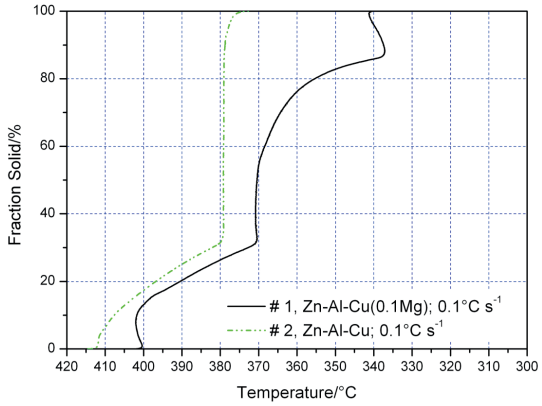

Fig. 12. Fraction solid during solidification of the individual components of the alloys cooled at a rate of 0.1°C s^{-1}

TABLE 3

Latent crystallization heat released by the crystallised phases, and its percentage of the entire alloy crystallization volume of the Zn-Al-Cu alloy, cooled at a rate of 0.1°C s^{-1}

Heat capacity in liquid state Cp_l, J (g·°C)$^{-1}$	Heat capacity in solid state Cp_s, J (g·°C)$^{-1}$		Sample mass, g
0.5305	0.4407		152.08
Transformation	Latent crystallisation heat		Percentage, %
	Samples, J	Mass of the samples, J g^{-1}	
L→ α	576.73	3.79	7.63
L→ $E_{(Zn+Al)}$	6723.56	44.53	92.37
total	7300.29	48.32	100

TABLE 4

Latent crystallization heat released by the crystallised phases, and its percentage of the entire alloy crystallization volume of the Zn-Al-Cu(0.1Mg) alloy, cooled at a rate of 0.1°C s^{-1}

Heat capacity in liquid state Cp_l, J (g·°C)$^{-1}$	Heat capacity in solid state Cp_s, J (g·°C)$^{-1}$		Sample mass, g
0.523	0.4362		151
Heat capacity in liquid state Cp_l, J (g·°C)$^{-1}$	Heat capacity in solid state Cp_s, J (g·°C)$^{-1}$		Percentage, %
	Samples, J	Mass of the samples, J g^{-1}	
L→ α	648.56	4.29	7.85
L→ $E_{(Zn+Al)}$	5975.04	39.57	77.85
L→ $EW_{(Zn+Al+Mg)}$	1006.82	6.67	14.3
total	7630.42	50.53	100

4. Summary and conclusions

The addition of Mg to the hypoeutectic alloy Zn-Al causes changes of the alloy structure and morphology of the eutectics and the obtained Zn phase. The addition of Mg causes also a decrease of the solidification start temperature T_L of 11°C and the temperature of the crystallisation end T_{Sol} of 32°C. It occurs also clear change of the solid fraction share between the alloys with and without Mg in the chemical composition (Fig. 12).

The monotectics visible in the SEM microstructure reveals a distance between the Zn and Al reach areas of ca 100nm, it seen to bee that this type of structure occurs only on th ealloy with magnesium addition, its amount in the total structure is hovewer very small and not detectable in the crystallisation curve, further TEM investigation can help to revael its nature and influence on the sourounding structure.

Acknowledgements

This publication was financed by the Ministry of Science and Higher Education of Poland as the statutory financial grant of the Faculty of Mechanical Engineering SUT.

REFERENCES

[1] L.J. Yang, J of Mat Proc Techn. **192–193**, 114–120 (2007).
[2] M. Krupinski, B. Krupinska, K. Labisz, Z. Rdzawski, W. Borek, J Therm Anal Calorim. **118** (2), 1361-1367 (2014).
[3] M. Krupinski, B. Krupinska, Z. Rdzawski, K. Labisz, T. Tanski, J Therm Anal Calorim. **120** (3), 1573-1583 (2015).
[4] T. Tanski, K. Labisz, B. Krupinska, M. Krupinski, M. Krol, R. Maniara, W. Borek, J Therm Anal Calorim. **123** (1), 63-74 (2016).
[5] A.E. Ares, L.M. Gassa, S.F. Gueijman, C.E. Schvezov, J of Crys Grow. **310**, 1355-1361 (2008).
[6] T.J. Chen, Y. Hao, J. Sun, Y.D. Li, Sci and Techn of Adv Mat. **4**, 495–502 (2003).
[7] M. Król, T. Tański, W. Sitek, Mater. Sci. Eng. **95** A,. 012006 (2015).
[8] W.T. Kierkus, J.H. Sokolowski, AFS Transactions 107, (1999).
[9] L. Liu, F. Liu, M. Zhu, Mater. **7**, 1173-1187 (2014).
[10] V. Raghavan, J of Phas Eq and Diff. **28**(2), 203-208 (2007).
[11] P. Liang, H.L. Su, P. Donnadieu, M.G. Harmelin, A. Quivy, P. Ochin, G. Effenberg, H.J. Seifert, H.L. Lukas, and F. Aldinger, Metallkd. **89** (8), 536-540 (1998).
[12] P. Liang, T. Tarfa, J.A. Robinson, S. Wagner, P. Ochin, M.G. Harmelin, H.J. Seifert, H.L. Lukas, and F. Aldinger, Thermochim. Acta **314**, 87-110 (1998).